Available online at www.sciencedirect.com
SCIENCE DIRECT®
International Journal of Heat and Mass Transfer 49 (2006) 287–296
International Journal of HEAT and MASS TRANSFER
www.elsevier.com/locate/ijhmt

A parametric study on the laminar flow in an alternating horizontal or vertical oval cross-section pipe with computational fluid dynamics

Wen-Lih Chen *, King-Leung Wong, Ching-Te Huang

Department of Mechanical Engineering, KSUT, 949, Da Wan Rd., Yung-Kang City, Tainan Hsien 710, Taiwan

Received 10 December 2004; received in revised form 1 July 2005
Available online 24 August 2005

Abstract

A parametric study, aiming to understand the effects of geometrical changes of an alternating horizontal or vertical oval cross-section pipe to its thermal performance, is presented. Three geometrical parameters are examined. The study is conducted by using computational fluid dynamics (CFD) and is focused on laminar flows only. The study shows that it is very difficult to find an optimized geometry which can perform well for a wide range of Reynolds numbers. However, the results indicate that the current pipe, if well designed, can still perform much better than a circular pipe at the flow conditions specified in this paper.

1. Introduction

Heat exchangers are used in a wide range of industrial as well as household devices, such as boilers, air conditioners, refrigerators, etc. Hence, to improve the performance of heat exchangers has been an active and important research subject, and enormous efforts have been made in the study of heat-transfer-improvement techniques [1–5]. Since circular pipes are widely used in heat-exchange devices such as tube bank in a boiler, evaporator in a refrigerator, and radiators in a heating system, to improve the heat-transfer performance of pipes has been an important research subject, and a variety of proposals have been offered in open literature including sinusoidal wavy surface, optimal variation of wall thickness, contraction–expansion–contraction pipe insertion, and many others [6–8]. These were proven to achieve a certain degree of improvement over pipe's thermal performance; however, some of them involved geometries, which were difficult to be manufactured or mass-produced. Guo et al. [9] proposed an experimentally verified theory called 'uniformity principle of temperature difference field', which states that the thermal performance of heat exchangers will be largely improved if higher degree of uniformity of temperature gradient can be achieved. Later Tao et al. [10] demonstrated that by reducing the angle between velocity and temperature gradient in the flow domain could effectively increase the heat flux occurring on the boundaries. According to Tao's theory, the problem associated with the heat transfer in a circular pipe can be readily explained. For laminar fully developed pipe flow, both in flow and temperature fields, the velocity vector becomes almost vertical to the temperature gradient; hence the field integration of the inner product of velocity and

* Corresponding author. Fax: +886 6 2050509.
E-mail address: wlchen@mail.ksut.edu.tw (W.-L. Chen).

0017-9310/$ - see front matter © 2005 Elsevier Ltd. All rights reserved.
doi:10.1016/j.ijheatmasstransfer.2005.07.005

Nomenclature

C_p	specific heat of fluid
d	diameter of a circular pipe
d_a, d_b	long and short diameters of an oval-cross-sectional pipe
f	friction coefficient of the alternating oval pipe
f_s	friction coefficient of circular pipe
g	gravity acceleration
l	the length of a sectional unit, including a transition section and a const cross-section-area section
l_t	the length of a transition section
n	direction normal to the wall
Nu	Nusselt number
Nu_d	averaged Nusselt number of the alternating oval pipe
Nu_s	averaged Nusselt number of circular pipe
p	pressure
q	heat flux
r_a, r_b	long and short radii of an oval-cross-sectional pipe
Re	Reynolds number
T	temperature
u, v, w	velocity components in x, y, and z directions, respectively
x, y, z	directions in Cartesian coordinates
k	fluid conductivity

Greek symbols

ρ	fluid density
μ	fluid dynamic viscosity
v	fluid kinematic viscosity

Subscripts

ave	averaged value
H	high temperature
L	low temperature
w	value on the wall

temperature gradient is very small. This would result in very small heat-transfer rate on pipe's wall since the first-order derivative of temperature on the wall in the radial direction is proportional to the field integration of velocity and temperature gradient's inner product. To solve this problem, measures need to be taken to offer a better coordination between velocity and temperature gradient. This led to the development of an alternating horizontal or vertical oval cross-section pipe [11] as shown in Fig. 1 for the purpose of heat-transfer enhancement. As seen, the entrance section of the pipe is circular with d in diameter. It is bridged to a horizontally positioned elliptical section by a transition section. This horizontal section is then connected to a vertically positioned elliptical section, again, via another transition section. The pattern of this alternating horizontal and vertical section arrangement is then repeated until end of the tube where the final section becomes circular again. Here, the long and short diameters of all elliptic sections are d_a and d_b, respectively, while the length of a sectional unit, including a transition section and a constant-area elliptic section, is l. This pipe creates secondary flows, which reduces the angle between velocity and temperature gradient and it enhances rate of heat transfer. Guo [11] measured that, at turbulent flows, this pipe could promote heat transfer up to 300% compared with a circular pipe with only a moderate penalty of increase in skin friction, ranging from 30% to 120%. This proved the favorable heat-transfer performance of such configuration. However, Guo's measurement, mainly focused on pipe's overall heat-transfer rate and pressure drop, did not include the details of the flow and temperature fields, and the paper also missed report on the most important geometrical factors contributing to heat-transfer enhancement. Therefore, the authors conducted numerical studies on both turbulent [12] and laminar [13] flows in Guo's geometry to shed some light into the complex 3D flow in the pipe. In the instance of laminar flow, Guo's configuration remarkably promotes rate of heat transfer 11 times the value of a circular pipe at $Re = 2000$ with six times increase in the level of skin friction. Of the special interest to engineers is the performance or the effectiveness of a pipe, which can be evaluated by the ratio between the rate of heat transfer and the magnitude of pressure drop. Using this standard, Guo's pipe generally achieves significant improvement over a circular pipe. On the other hand, the improvement becomes marginal when the flow becomes turbulent. In both laminar and turbulent flows, the computation showed that there were large axial separation bubbles in the transition section whenever the magnitude of the increase on pressure drop was large. This seems to suggest that the axial separation bubbles are responsible for the dramatic increase on the level of pressure drop, and the effectiveness of the alternating horizontal or vertical oval cross-section pipe could be improved by reducing the size of these separation bubbles. This motivates us to conduct a parametric study to find better geometries, which can preserve the pipe's favorable heat-transfer performance and reduce the level of pressure drop. In the present study, the focus is on laminar flows with Reynolds number no greater than 2000. The problem associated with turbulence flows will be addressed in some future papers.

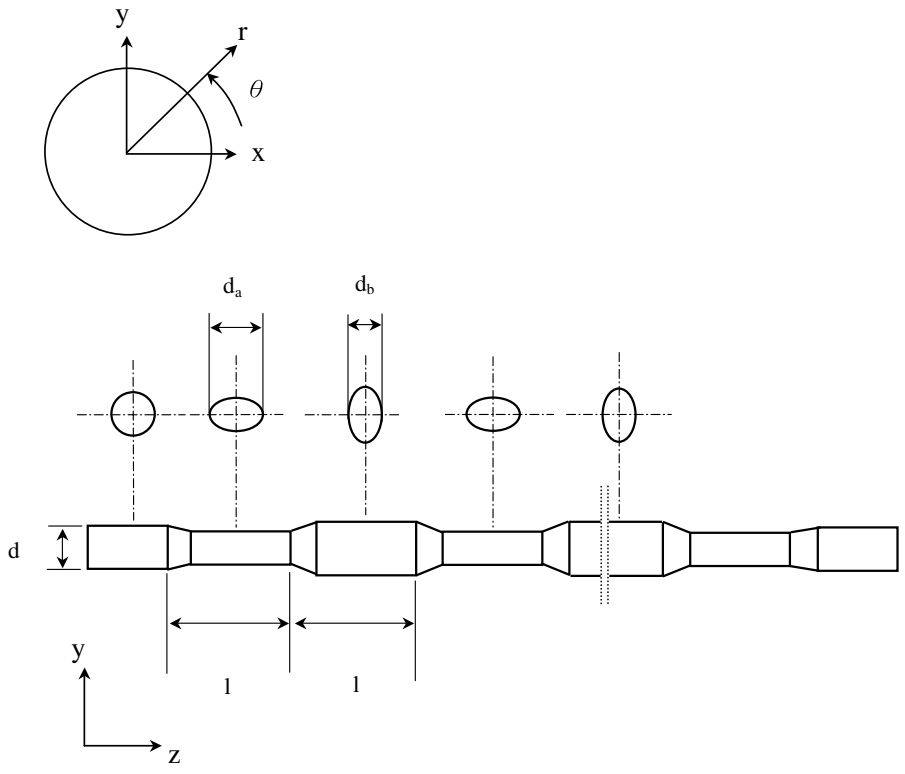

Fig. 1. The geometry of the alternating horizontal or vertical oval cross-section pipe.

2. Physical model

The steady-state three-dimensional mass conservation, Navier–Stokes, and energy conservation governing equations can be written as

Continuity equation

$$\frac{\partial}{\partial x}(\rho u)+\frac{\partial}{\partial y}(\rho v)+\frac{\partial}{\partial z}(\rho w)=0 \tag{1}$$

Momentum equation

$$\rho\left(u\frac{\partial u}{\partial x}+v\frac{\partial u}{\partial y}+w\frac{\partial u}{\partial z}\right)=-\frac{\partial p}{\partial x}+\rho g_x+\frac{\partial}{\partial x}\left(\mu\frac{\partial u}{\partial x}\right)+\frac{\partial}{\partial y}\left(\mu\frac{\partial u}{\partial y}\right)+\frac{\partial}{\partial z}\left(\mu\frac{\partial u}{\partial z}\right) \tag{2}$$

$$\rho\left(u\frac{\partial v}{\partial x}+v\frac{\partial v}{\partial y}+w\frac{\partial v}{\partial z}\right)=-\frac{\partial p}{\partial y}+\rho g_y+\frac{\partial}{\partial x}\left(\mu\frac{\partial v}{\partial x}\right)+\frac{\partial}{\partial y}\left(\mu\frac{\partial v}{\partial y}\right)+\frac{\partial}{\partial z}\left(\mu\frac{\partial v}{\partial z}\right) \tag{3}$$

$$\rho\left(u\frac{\partial w}{\partial x}+v\frac{\partial w}{\partial y}+w\frac{\partial w}{\partial z}\right)=-\frac{\partial p}{\partial z}+\rho g_z+\frac{\partial}{\partial x}\left(\mu\frac{\partial w}{\partial x}\right)+\frac{\partial}{\partial y}\left(\mu\frac{\partial w}{\partial y}\right)+\frac{\partial}{\partial z}\left(\mu\frac{\partial w}{\partial z}\right) \tag{4}$$

Energy equation

$$\rho c_p\left(u\frac{\partial T}{\partial x}+v\frac{\partial T}{\partial y}+w\frac{\partial T}{\partial z}\right)=\frac{\partial}{\partial x}\left(k\frac{\partial T}{\partial x}\right)+\frac{\partial}{\partial y}\left(k\frac{\partial T}{\partial y}\right)+\frac{\partial}{\partial z}\left(k\frac{\partial T}{\partial z}\right) \tag{5}$$

In Guo's measurement, the working fluid was water, and the difference between the maximum and minimum temperature was less than 30 degree. Under this circumstance, all fluid properties ρ, μ, C_p could be assumed to be constants. In addition, the effect of body force in the momentum equation is small and can be omitted. The boundary conditions are (according to Fig. 1):

At inlet

$$u=v=0,\quad w=w_0,\quad T=T_{\mathrm{H}} \tag{6}$$

At outlet

$$\frac{\partial u}{\partial z}=\frac{\partial v}{\partial z}=\frac{\partial w}{\partial z}=\frac{\partial T}{\partial z}=0 \tag{7}$$

On the wall

$$u=v=w=0,\quad T=T_{\mathrm{L}} \tag{8}$$

In Eqs. (6) and (8), T_{H} and T_{L} are high and low temperatures, respectively. The use of constant wall

temperature in Eq. (8) seems to oversimplify the wall conditions in practical applications, where the temperature field outside the pipe might interact with that inside the pipe, and create much more complicated wall conditions than constant wall temperature. Hence, the results reported in this paper can only be applied to those flows with nearly constant wall temperatures.

3. Numerical framework

Calculation reported herein have been performed with the unstructured-mesh, fully collocated, finite-volume code, 'USTREAM' developed by the first named author. This is the descendent of the structured-mesh, multi-block code of 'STREAM' [14]. Convection of mean-flow as well as turbulence quantities is approximated with the scheme 'UMIST' [15], a second-order TVD implementation of the QUICK scheme of Leonard [16]. Within this scheme, the transport solutions and the pressure-correction equation are solved sequentially and iterated to convergence, defined by reference to Euclidean residual norms for mass, the moment components and the temperature. A fully implicit scheme, with the time variation approximated to second-order accuracy, is incorporated to solve unsteady problems.

4. Results and discussion

In Guo's experiment, the values of d, d_a, d_b, l and the length of a transition section l_t were 16.5 mm, 20 mm, 13 mm, 40 mm and 6 mm, respectively. The Reynolds number Re is defined according to the geometry of the initial circular-cross-section as $\frac{w_0 d}{\nu}$. This makes the entrance flow condition identical to a pure-circular pipe at the same Reynolds number thus facilitates the comparison of the heat-transfer performance between the alternating horizontal or vertical oval cross-section oval pipe and its circular counterpart. Since this paper only concerns laminar flow, the Reynolds number investigated ranges from 500 to 2000, where the later value is normally considered as the upper limit of the flow remaining laminar in a circular pipe. Computation showed that both flow and temperature fields become periodical before the sixth sectional unit, hence, the final computational domain comprises nine sectional units, among which the eighth unit is taken for the analytical purpose. The mesh size used in this paper is $80 \times 20 \times 330$ in radial, circumferential, and axial directions, respectively. The associated grid-independence test has been conducted and reported in [13], and there is no need to document the details here.

To assess the accuracy of the present calculation, the predicted variations of overall Nusselt number and friction coefficient with Guo's original pipe are compared with the experimental data in Fig. 2(a) and (b). Here, Nusselt number is calculated as follows:

$$Nu = \frac{q_w}{T_{ave}} \frac{d}{\kappa} \tag{9}$$

where q_w, T_{ave} and κ are the wall heat flux, sectional averaged temperature and wall conductivity, respectively. Wall heat flux q_w is calculated as $q_w = \kappa \frac{\partial T}{\partial n}$, in which n is the normal direction from the wall surface. The averaged Nusselt number from a fully developed laminar circular-pipe flow, a constant value of 3.66, is also given in the plot. This value, well documented in a number of heat-transfer textbooks [17], is independent of Reynolds number as long as the flow remains laminar. In addition to producing the experimental data, Guo also performed computation with commercial CFD code FLUENT, and the results are also cross-plot-

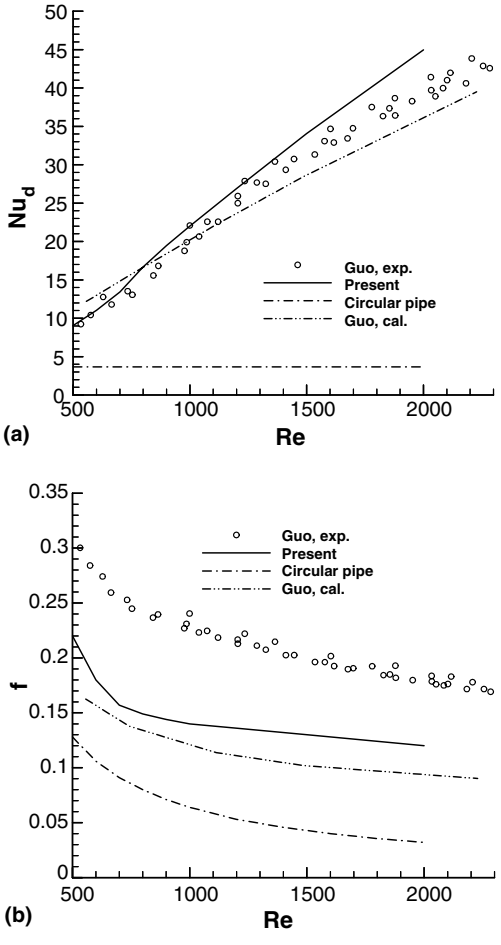

Fig. 2. The distributions of averaged Nusselt numbers and friction coefficients of the alternating horizontal or vertical oval cross-section pipe and circular pipe: (a) Nusselt numbers and (b) friction coefficients.

ted in Fig. 2. As seen, the present calculation slightly over predicts the Nusselt number at high Reynolds number, while Guo's computation slightly under predicts this quantity. But both results are in good agreement with the data. Since the friction coefficient is in proportion to pressure drop, one can estimate it by calculating the friction coefficient as follows:

$$f = \frac{\Delta p}{\frac{1}{2}\rho u_0^2}\frac{d}{l} \tag{10}$$

where Δp is the pressure difference at the inlet and outlet of a sectional unit. The friction coefficient in circular pipe is estimated from the following well-known equation for laminar flows:

$$f_s = 64/Re \tag{11}$$

It is noticeable that compared to the measurement, both the present and Guo's calculations generally underestimates the level of friction coefficient. The reason for this discrepancy is not clear. It is unlikely to be a numerical problem since by testing runs for $Re = 100$–900, the current numerical procedure is able to return circular-pipe friction coefficients which are within 1% difference with the values specified by Eq. (11). In contrast to Guo's numerical results, the present results seem to be in better agreement with the data, both quantitatively and qualitatively. In a brief summary, this exercise shows that the present calculation predicts well in terms of the averaged Nusselt number but underestimates the magnitude of friction coefficient.

The heat-transfer performance of Guo's original pipe has been well discussed in [13], and there is no need to re-document it here. However, to convey the idea of why three different geometric parameters are selected for investigation in this paper; some major conclusions are recited here. Compared to a circular pipe, at $Re = 2000$, Guo's configuration can achieve 10 times larger heat-transfer rate while the increase on the friction-coefficient level is about six times. This has already been a significant improvement over circular-pipe's performance. Fig. 3 depicts the variations of Nusselt number and averaged pressure along the axial direction at $Re = 1000$. Here, the value of the axial variation of the pipe's cross-section area is also plotted to serve as an indication of where the transition section is located. As shown in Fig. 3(a), the axial Nusselt number distributions indicate that the increase on heat-transfer rate is largely attributed to the transitional sections, which raise the level of heat transfer at some fixed locations along the pipe. However, the distributions of averaged pressure given in Fig. 3(b) suggest that they are responsible to most of the pressure drop. Obviously, the transition sections are of great importance to the overall performance of this pipe. As a result, all the geometric parameters associated with transition section need to be investigated. These include the ratio between the oval's

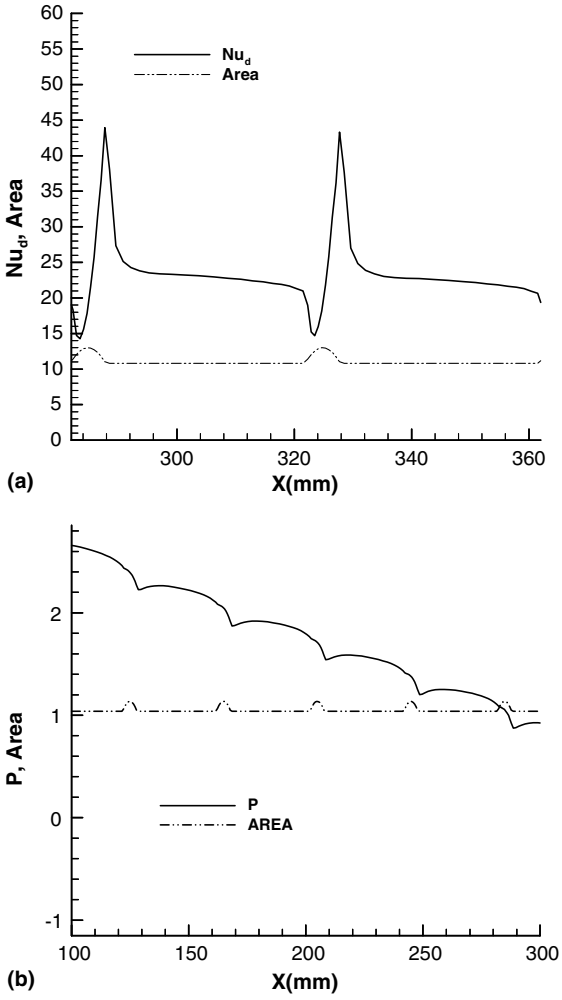

Fig. 3. The distributions of Nusselt number and averaged pressure along the alternating horizontal or vertical oval cross-section pipe's axial direction at $Re = 1000$: (a) Nusselt numbers and (b) average pressure.

long and short radii $\frac{r_a}{r_b}$ and the length of a transition section l_t. Apart from the two parameters concerning the transition sections; Fig. 3(a) seems to imply that by shortening the length of a sectional unit l i.e. letting the transition sections appear more frequently along the pipe, would further improve the overall heat-transfer rate. Consequently, the parameter l is also selected for investigation. In summary, the effects of three geometric parameters, namely $\frac{r_a}{r_b}$, l_t, and l, are examined in this paper.

Three different Reynolds numbers, 500, 1000, and 2000, respectively, representing low, medium, and high Reynolds number are adopted for the current investigation. Furthermore, as shown in Table 1, each parameter has eight different values. This means that there are typically 24 cases for any individual case group. However, a

Table 1
The values used for the three different parameters

	1	2	3	4	5	6	7	8
r_a/r_b ($l_t = 6$ mm, $l = 40$ mm)	1.2	1.35	1.44	1.53	1.64	1.75	1.87	2.0
l_t, mm ($r_a/r_b = 1.64$, $l = 40$ mm)	6	8	10	12	14	16	18	20
l, mm ($r_a/r_b = 1.64$, $l_t = 6$ mm)	12	16	20	24	28	32	36	40

small portion of cases do not yield a stable solution at high Reynolds number, hence their results are not included. In the following, the effects of changing these parameters will be discussed separately.

4.1. The effects of $\frac{r_a}{r_b}$

As detailed in Table 1, the value of $\frac{r_a}{r_b}$ investigated in this paper is in the range from 1.2 to 2.0. In this group of cases, two did not return stable solutions, namely $\frac{r_a}{r_b} = 1.87$ and 2.0 at $Re = 2000$. Here, the higher the value of $\frac{r_a}{r_b}$ is, the flatter an oval section becomes, signifying that the degree of geometrical contraction and expansion at the transition sections is more drastic. This would result in an increase on both the amounts of Nusselt number and friction coefficient due to extremer geometrical changes at the transition sections. The variations of Nusselt number and friction coefficients versus $\frac{r_a}{r_b}$ are given in Fig. 4. As expected, both quantities show tendency of increase as the value of $\frac{r_a}{r_b}$ rises. In terms of the Nusselt number distributions in Fig. 4(a), a general tendency of all lines' variation can be described as: a gentler ascending at low $\frac{r_a}{r_b}$ then followed by a steeper one at medium $\frac{r_a}{r_b}$, and finally the slope becomes tender again at high $\frac{r_a}{r_b}$. That is, there is a range of $\frac{r_a}{r_b}$, where Nusselt number would react more sensitively to the changes of $\frac{r_a}{r_b}$. This range is located at lower $\frac{r_a}{r_b}$ scale for $Re = 2000$ and at higher scale for $Re = 500$. Regarding to the variations of friction coefficients in Fig. 4(b), all lines demonstrate that the slope becomes steeper as the $\frac{r_a}{r_b}$ value increases, denoting a rapid rise on the level of pressure drop at high value of $\frac{r_a}{r_b}$.

To evaluate the performance, or effectiveness, of the current pipe, we use a performance factor $(Nu_d/Nu_s)/(f/f_s)$, where Nu_s and f_s respectively stand for Nusselt number and friction coefficient in a circular pipe at the same flow conditions as the current pipe. This factor is essentially the ratio between the magnitudes of heat-transfer rate enhancement and the friction-coefficient increase. Hence, the larger this factor is, the better the tube's performance becomes. Fig. 5 shows the variations of this factor. From the plot, one can see that the performance of the alternating horizontal or vertical oval cross-section pipe varies quite differently at different Reynolds numbers. At low Reynolds number ($Re = 500$), it tends to perform well at radical geometrical changes in the transition sections. In contrast, it can only do well at milder geometrical changes at high Reynolds number

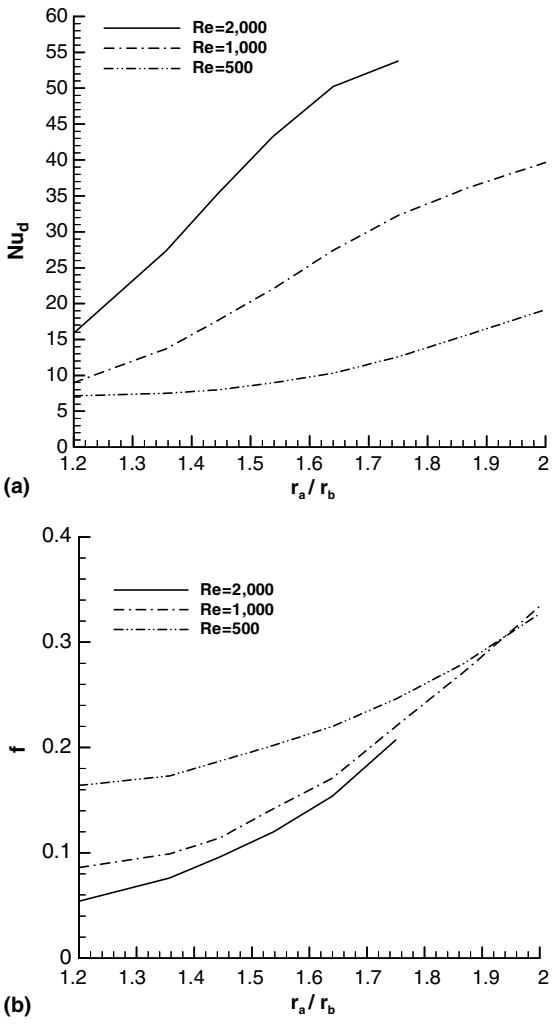

Fig. 4. The variations of averaged Nusselt number and friction coefficient versus $\frac{r_a}{r_b}$ at different Reynolds numbers ($l = 40$ mm, $l_t = 6$ mm): (a) Nusselt numbers and (b) friction coefficients.

($Re = 2000$). According to the plot, one can estimate that an alternating horizontal or vertical oval cross-section pipe would have better performance if its $\frac{r_a}{r_b}$ value is in the range from 1.44 to 1.64 for the Reynolds numbers examined in this paper. Nevertheless, considering the fact that the yielded Nusselt number is much higher at $\frac{r_a}{r_b} = 1.64$ than that at $\frac{r_a}{r_b} = 1.44$, we fix the value of $\frac{r_a}{r_b}$ as 1.64 when conduct the rest two parametric investigations.

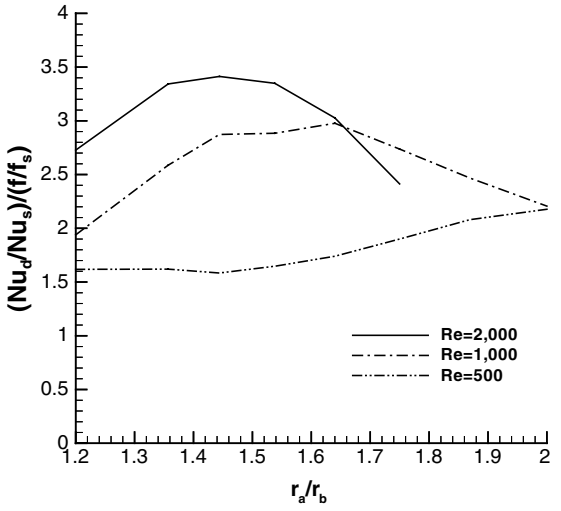

Fig. 5. The variations of the performance factor versus $\frac{r_a}{r_b}$ at different Reynolds numbers.

4.2. The effects of l_t

In addition to the aforementioned fixed $\frac{r_a}{r_b}$ value, the length of a sectional unit is also fixed at 40 mm in this group of cases. The longer the transition sections become, the less severe their geometrical contraction and expansion are. This would result in a smaller degree of adverse pressure gradient at the expansion part of the transition sections, and hence reduce the sizes of axial separation bubbles. Therefore, the main purpose of performing this set of test cases is to see whether elongating the transition sections can actually be beneficial to the reduction of pressure loss, especially at high Reynolds numbers. Here, all cases yield stable solutions, allowing us to examine the effects of l_t in full spectrum.

Again, we discuss the effects of l_t through the distributions of Nusselt number, friction coefficient, and the performance factor, and they are plotted in Fig. 6(a), (b), and Fig. 7, respectively. The distributions of Nusselt number and friction coefficient all show a tendency of descending as the value of l_t increases. Although elongating the transition sections indeed reduces friction, the undesired effect is the diminishing of the rate of heat transfer. This is because the degree of geometrical contraction at the transition sections, which is the main factor of promoting heat transfer, is also reduced as the transition sections get stretched. Now the remaining issue is to see which one declines faster. This can be readily evaluated from the distributions of performance factor in Fig. 7. The plot shows that this quantity is relatively flat for $Re = 500$ and 1000, indicating that both friction coefficient and Nusselt number are declining at similar rate. In contrast, the line for $Re = 2000$ reveals a peak near $l_t = 14$ mm, and there is a significant difference between the minimum and maximum values. Here, the minimum value is located at $l_t = 6$ mm, which is one of the original geometrical measures in Guo's configuration. This has clearly demonstrated that by elongating the transitions section can improve the effectiveness of the pipe at high Reynolds number. The reason why it is particularly beneficial to pipe's performance at high Reynolds number is because the axial separation bubble at $Re = 2000$ is very large, occupying a major portion of the expanding part of the transition section and extending to some distance downstream into the constant-area section (see [13]). The separation bubble then decreases in size dramatically with the increase on l_t, especially in the range between $l_t = 6$ mm and 10 mm. It becomes very small when l_t is larger than 14 mm. In Fig. 6(b),

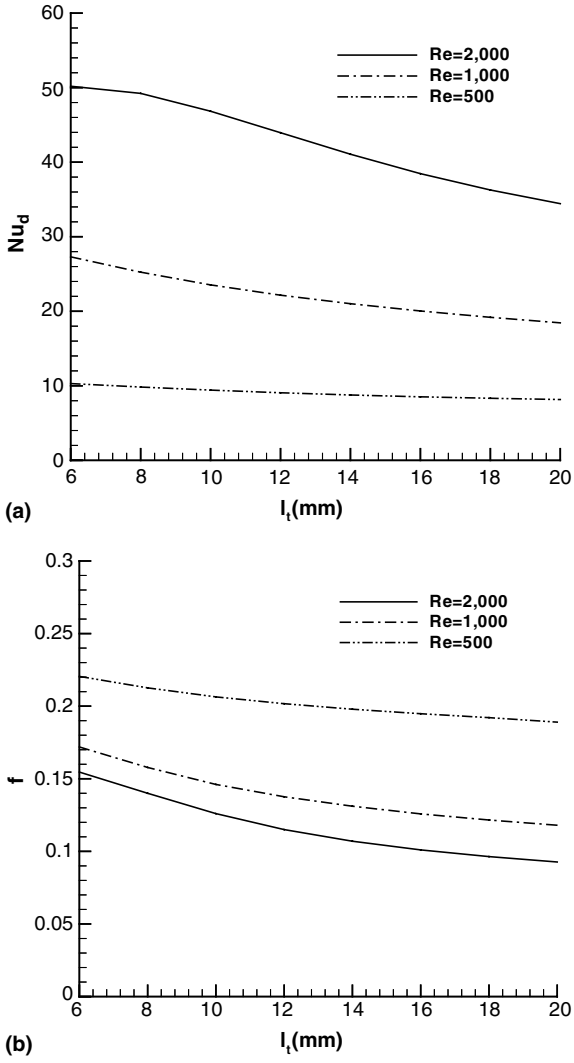

Fig. 6. The variations of averaged Nusselt numbers and friction coefficients versus l_t at different Reynolds numbers ($l = 40$ mm, $\frac{r_a}{r_b} = 1.64$): (a) Nusselt numbers and (b) friction coefficients.

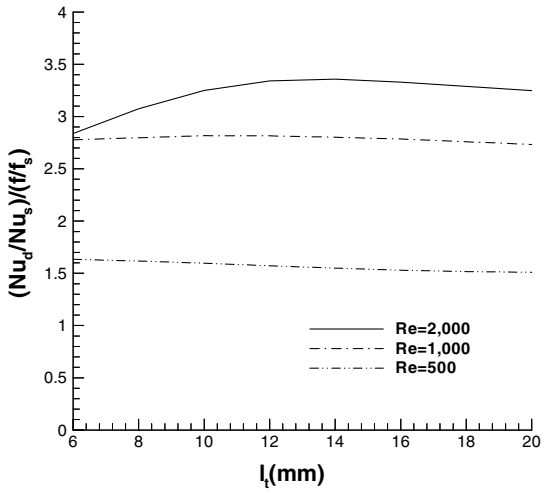

Fig. 7. The variations of the performance factor versus l_t at different Reynolds numbers.

one can see that the friction coefficient for $Re = 2000$ declines rapidly in the range between $l_t = 6$ mm and 10 mm then it declines much gentler when $l_t \geqq 14$ mm. That is, fast decline on friction coefficient corresponds to rapid reduction in the size of the separation bubble. A similar behavior is also observed for $Re = 1000$. In terms of $Re = 500$, the size of the separation bubble is already very small at $l_t = 6$ mm, and it almost disappears when $l_t \geqq 8$ mm. The distinct decline rates observed in $Re = 2000$ becomes much less pronounced in the friction-coefficient distributions, which seems to be more linear, for $Re = 500$ (see Fig. 6(b)). Although it is very difficult to calculate the percentage of pressure drop contributed by the separation bubble, from the above observations, it is reasonable to argue that the size of the separation bubble plays a very important role on the magnitude of friction coefficient. A slight reduction in the separation bubble size can significantly reduce the pressure drop, hence improving the pipe's performance.

4.3. The effects of l

In this group of test cases, $\frac{r_a}{r_b}$ and l_t are fixed at 1.64 and 6 mm, respectively. Under this circumstance, shortening the length of unit sections literally raises the length, in percentage, of the transition section with respect to a sectional unit. Since the transition section is the major contributor to the enhancement of heat transfer, this is expected to increase the overall heat-transfer rate of the pipe. Unfortunately, the level of friction coefficient will be increased due to the same reason. In this group, the length of a sectional unit is shortened gradually from the original length of 40 mm to 12 mm, in which the percentage of the transition section of the shortest one reaches 50% of the total length of a sectional unit. In this group, there are two cases failing to return stable solutions, namely $l = 12$ mm and 16 mm for $Re = 2000$.

Again, the discussions here will be based on the distributions of Nusselt number, friction coefficient, and the performance factor, which are depicted respectively in Fig. 8(a), (b), and Fig. 9. In terms of heat-transfer enhancement, an astonishing result can be seen in Fig. 8(a), which indicates that Nusselt number can reach a value higher than 70 for $l = 20$ mm and $Re = 2000$. This is an increase of more than 20-folds when compared with that for a circular pipe. Additionally, there are also significant increases on the magnitude of Nusselt number for the other two Reynolds numbers when l is reduced. This proves that, while fixing the length of the transition section, reducing the overall length of a sectional unit is

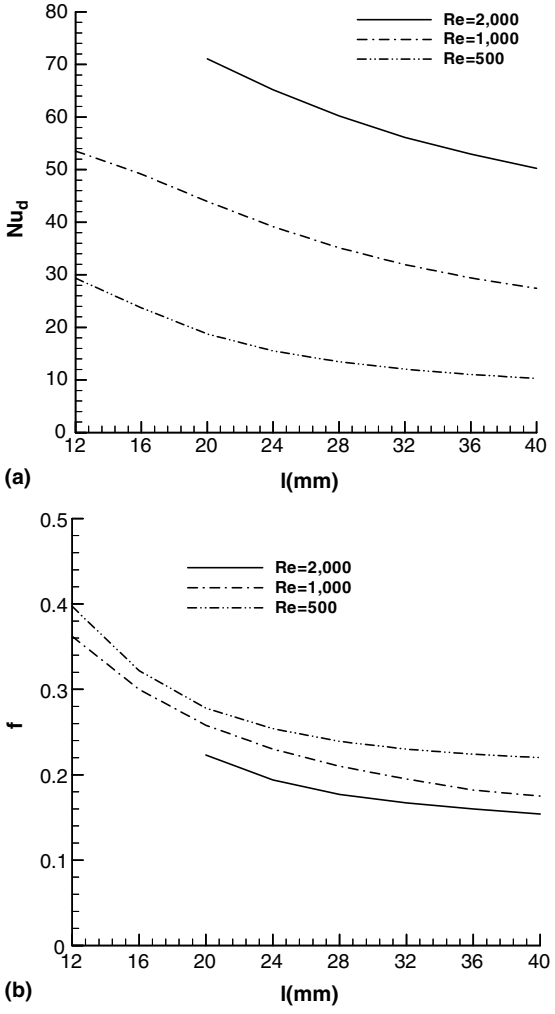

Fig. 8. The variations of averaged Nusselt numbers and friction coefficients versus l at different Reynolds numbers ($l_t = 6$ mm, $\frac{r_a}{r_b} = 1.64$): (a) Nusselt numbers and (b) friction coefficients.

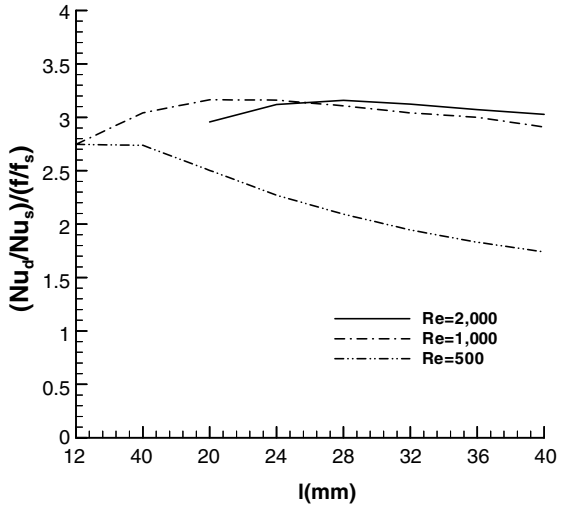

Fig. 9. The variations of the performance factor versus l at different Reynolds numbers.

indeed a very effective way to promote heat transfer. However, the similar problem discussed in the previous sub-sections also occurs here: a gain on the magnitude of Nusselt number is normally accompanied by an increase in the pressure drop. Fig. 8(b) shows that the slope of friction is especially steep at small l, where the gain in Nusselt number is most significant. To balance the gain in heat transfer and the loss of pressure, one needs to see the distributions of the performance factor given in Fig. 9. As seen, for all Reynolds numbers, the variation of this quantity is moderate over the range of l investigated. Nevertheless, it is still noticeable that the ratio has maximum values at $l = 28$ mm for $Re = 2000$ and $l = 20$ mm for $Re = 1000$, respectively. In terms of $Re = 500$, it seems that the performance factor does not reach the maximum value yet even at the lower limit of $l = 12$ mm. This is an echo to the observation in the parametric investigation of $\frac{r_a}{r_b}$, which again demonstrates that the alternating horizontal or vertical oval cross-section pipe performs well at radical geometrical changes at low Reynolds number, while it can only do so at moderate geometrical changes at high Reynolds numbers.

5. Conclusions

A numerical parametric study has been conducted to investigate the effects of three geometrical parameters on the heat-transfer performance in an alternating horizontal or vertical oval cross-section pipe. The parameters examined are the ratio between oval's long and short radii $\frac{r_a}{r_b}$, the length of a transition section l_t, and the length of a sectional unit l. The main conclusions can be summarized as follows:

1. Both Nusselt number and friction-coefficient increase as the value of $\frac{r_a}{r_b}$ rises. However, regarding the effectiveness of the pipe, which is evaluated by the ratio between the magnitudes of increases in Nusselt number and friction coefficient, the calculations show that at low Reynolds number, the pipe can have better performance at high $\frac{r_a}{r_b}$ value (2.0 for $Re = 500$) but at high Reynolds number, it can only do so at moderate $\frac{r_a}{r_b}$ value (1.44 for $Re = 2000$).
2. While fixing the values of l (at 40 mm) and $\frac{r_a}{r_b}$ (at 1.64), stretching the transition section will reduce both the magnitudes of Nusselt number and friction coefficient. Here, the performance factor indicates that the pipe reaches its maximum effectiveness at $l_t = 14$ mm for $Re = 2000$. For $Re = 1000$ and 500, the variation of l_t seems to pose little influence on the effectiveness of the pipe.
3. When both the values of l_t and $\frac{r_a}{r_b}$ are fixed, shortening the length of a sectional unit is a very effective way to enhance heat transfer. Here, the Nusselt number reaches a staggering high level of 74 at $l = 20$ mm and $Re = 2000$. Unfortunately, the gain on the Nusselt number is compromised by the steep rise of friction coefficient. The distributions of the performance factor demonstrate that the best balance between the two is at $l = 28$ mm, 20 mm, and 12 mm for $Re = 2000$, 1000 and 500, respectively. This again shows that the performance of the alternating horizontal or vertical oval cross-section pipe varies quite widely at different Reynolds number.

From the above conclusions, one can realize that it is very difficult to design an alternating horizontal or vertical oval cross-section pipe which will perform equally well at a wide range of Reynolds numbers. It is only possible to come up with an optimized design at a fixed Reynolds number, and the study conducted here has provided very useful information to accomplish that.

Acknowledgements

The work reported herein was supported by a Taiwanese National Science Council funded project, numbered NSC-93-2212-E-168-004. The authors are grateful for this support.

References

[1] B.S. Petukhov, V.N. Popov, Theoretical calculation of heat exchange and frictional resistance in turbulent flow in tubes of an incompressible fluid with variable physical properties, High Temp. Heat Phys. 1 (1963) 69–83.
[2] P. Kumar, R.L. Judd, Heat transfer with coiled wire turbulence promoters, Can. J. Chem. Eng. 48 (1970) 378–383.

[3] R.L. Webb, in: Principles of Enhanced Heat Transfer, John Wiley & Sons Inc., New York, 1994, p. 89.
[4] Y. Fujita, A.M. Lopez, Heat-transfer enhancement of twisted-tap inserts in turbulent pipe flows, Heat Transfer—Jpn. Res. 24 (1995) 378–396.
[5] A.E. Bergles, Heat transfer enhancement—the measuring of the second-generation heat transfer technology, Heat Transfer Eng. 18 (1997) 47–55.
[6] G. Russ, H. Beer, Heat transfer and flow field in a pipe with sinusoidal wavy surface—I. Numerical investigation, Int. J. Heat Mass Transfer 45 (1997) 1061–1070.
[7] M.E. Arici, Determination and use of the optimal variation of pipe wall thickness for laminar forced convection heat transfer, Int. Commun. Heat Mass Transfer 29 (2002) 663–672.
[8] H.F. Oztop, I. Dagtekin, Enhancement of heat transfer in a pipe with inner contraction–expansion–contraction pipe insertion, Int. Commun. Heat Mass Transfer 30 (2003) 1157–1168.
[9] Z.Y. Guo, S.Q. Zhou, Z.X. Li, L.G. Chen, Theoretical analysis and experimental confirmation of the uniformity principle of temperature difference field in heat exchanger, Int. J. Heat Mass Transfer 45 (2002) 2119–2127.
[10] W.Q. Tao, Z.Y. Guo, B.X. Wang, Field synergy principle for enhancing convective heat transfer—its extension and numerical verifications, Int. J. Heat Mass Transfer 45 (2002) 3849–3856.
[11] Z.Y. Guo, A brief introduction to a novel heat-transfer enhancement heat exchanger, internal report, Dept. of EMEMKLEHTEC, Tsinghua University, Beijing, China, 2003.
[12] W.L. Chen, Z. Guo, C.K. Chen, A numerical study on the flow over a novel tube for heat-transfer enhancement with a linear eddy-viscosity model, Int. J. Heat Mass Transfer 45 (2004) 3431–3439.
[13] W.L. Chen, L.C. Fang, A numerical study on the flow over a staggered oval pipe for heat-transfer enhancement, J. CSME 25 (2004) 209–216.
[14] F.S. Lien, W.L. Chen, M.A. Leschziner, A multiblock implementation of a non-orthogonal, collocated finite volume algorithm for complex turbulent flows, Int. J. Numer. Methods Fluids 23 (1996) 567–588.
[15] F.S. Lien, M.A. Leschziner, Upstream monotonic interpolation for scalar transport with application to complex turbulent flows, Int. J. Numer. Methods Fluids 19 (1994) 527.
[16] B.P. Leonard, A stable and accurate convective modeling procedure based on quadratic upstream interpolation, Comput. Methods Appl. Mech. Eng. 19 (1979) 59.
[17] I. DeWitt, Fundamentals of Heat and Mass Transfer, forth ed., Wiley, 1996, pp. 420–422.